Journal of Zhejiang University-SCIENCE B (Biomedicine & Biotechnology)
ISSN 1673-1581 (Print); ISSN 1862-1783 (Online)
www.jzus.zju.edu.cn; www.springerlink.com
E-mail: jzus@zju.edu.cn

Adhesion of bone marrow mesenchymal stem cells on porous titanium surfaces with strontium-doped hydroxyapatite coating*

Dan-li FU[1], Qiao-hong JIANG[1], Fu-ming HE[2], Bai-ping FU[†‡3]

([1]*Department of General Dentistry, West Branch of Stomatology Hospital, School of Medicine, Zhejiang University, Hangzhou 310006, China*)

([2]*Department of Oral Implantology, Stomatology Hospital, School of Medicine, Zhejiang University, Hangzhou 310006, China*)

([3]*Department of Prosthodontics, Stomatology Hospital, School of Medicine, Zhejiang University, Hangzhou 310006, China*)

[†]E-mail: fbp@zju.edu.cn

Received Nov. 16, 2016; Revision accepted Dec. 16, 2016; Crosschecked Aug. 16, 2017

Abstract: Objective: To determine the adhesion behavior of bone marrow mesenchymal stem cells (MSCs) on a titanium surface with a nanostructured strontium-doped hydroxyapatite (Sr-HA) coating. Methods: Sr-HA coatings were applied on roughened titanium surfaces using an electrochemical deposition method. Primary cultured rat MSCs were seeded onto Sr-HA-, HA-coated titanium, and roughened titanium surfaces, and they were then cultured for 1, 6, and 24 h. 3-(4,5-Dimethylthiazol-2-yl)-2,5-diphenyltetrazolium bromide (MTT) assay was used to determine the metabolic condition of the cells. Scanning electron microscopy (SEM) was used to observe the cell morphology. The cytoskeletal structure was analyzed using fluorescence actin staining to characterize cell adherence. Quantitative real-time reverse transcription polymerase chain reaction (RT-qPCR) was used to analyze the gene expression levels of FAK (focal adhesion kinase), vinculin, integrin β1, and integrin β3 after culturing for 24, 48, and 72 h. Results: MSCs cultured on the Sr-HA surface showed better cell proliferation and viability. Improvement of cell adhesion and structural rearrangement of the cytoskeleton were observed on the Sr-HA surface. The gene expression of FAK, vinculin, integrin β1, and integrin β3 was also elevated on the Sr-HA surface. Conclusions: Cell viability, adhesion, cell morphology, and the cytoskeletal structure were all upregulated considerably by the titanium surface modified with a Sr-HA coating.

Key words: Cell adhesion; Bone marrow mesenchymal stem cell; Strontium-doped hydroxyapatite; Titanium
http://dx.doi.org/10.1631/jzus.B1600517 **CLC number:** R783.1

1 Introduction

Titanium has been widely used as a biomaterial because of its excellent biocompatibility and osseointegration at the bone-implant interface (Branemark, 1983; Fage *et al.*, 2016).

In order to accomplish good osseointegration, the recruitment of osteogenic cells such as osteoblasts and mesenchymal stem cells (MSCs) is essential. Adhesion of the cells is the first stage of the interactions between the cells and implants after a biomaterial implantation, which consists of four steps: protein adsorption, cell–material contact, attachment, and spreading (Anselme, 2000; Uccelli *et al.*, 2008). It has been proven that the quality of adhesion is critical in modulating the capacity of a cell to proliferate and differentiate (Matschegewski *et al.*, 2010; Yim *et al.*, 2010; Seo *et al.*, 2013). It is widely accepted that MSCs are the first cells to colonize the implant surface. MSCs undergo osteoblastic differentiation in response to the microstructure of the titanium surface. Some studies suggest that the recognition is mediated by integrin receptors, and the integrin signaling is responsible for surface-dependent osteoblastic maturation (Krause *et al.*, 2000; Krishna

‡ Corresponding author

* Project supported by the Zhejiang Provincial Natural Science Foundation of China (No. LQ13H140001)

ORCID: Dan-li FU, http://orcid.org/0000-0001-8806-1729

et al., 2011; Dalby *et al.*, 2014; Kaneko *et al.*, 2014). Osteoblasts originate from bone marrow MSCs, so the commitment and differentiation of MSCs towards osteoblast lineage play an essential role in bone formation (Yang *et al.*, 2015).

Cell–material interactions are dictated by the surface properties of the material, such as chemical composition, micro/nano topography, roughness, and surface energy (Khang *et al.*, 2012; Zhao *et al.*, 2012; Zhou *et al.*, 2013; Sisti *et al.*, 2015). Previous studies demonstrated that cell adhesion could be influenced by three-dimensional (3D) nanotopography of the surface (Kuo *et al.*, 2012; Liu *et al.*, 2012). Compared to the 2D counterparts, gold-coated silicon nanopillars and ZnO nanoflowers improved cell adhesion. However, conflicting results have been reported that randomly oriented and upright crystallites of ZnO and SiO_2 inhibited cells' adhesion and spreading (Lee *et al.*, 2009; Loya *et al.*, 2010; Park *et al.*, 2010; Brammer *et al.*, 2011). Several studies have been undertaken to modify and improve the surface of titanium by synthesizing a nanostructured bioactive material such as hydroxyapatite (HA) coating, which would favor positive interactions with osteogenic cells (Shi *et al.*, 2013; Zhao *et al.*, 2014; Sirin *et al.*, 2015; Kumar *et al.*, 2016). In order to improve the osteo-conductivity, strontium (Sr) has been introduced into HA to improve the bone–tissue response to the material (Fu *et al.*, 2012; Jiang *et al.*, 2015). Sr increases osteoblast replication, differentiation, and bone matrix mineralization. On the other hand, Sr can reduce the osteoclast differentiation and resorbing activity. Sr has also been recently reported to direct the MSCs' commitment to the bone lineage (Peng *et al.*, 2009; Braux *et al.*, 2011; Yang *et al.*, 2011).

In recent years, many studies have highlighted the fabrication of strontium-doped hydroxyapatite (Sr-HA) on roughened implant surfaces (Aina *et al.*, 2013; Gao *et al.*, 2016; Tao *et al.*, 2016a). The electrochemical method is capable of depositing Sr into or onto HA to form rod-like HA crystallites with a hexagonal cross section and diameters of about 90 nm, similar to the structure of bone HA (Jiao and Wang, 2009). Recently, we demonstrated that the Sr-HA coating has the potential to enhance implant osseointegration (Fu *et al*., 2012).

Given the absence of data on the exact mechanism of how Sr-HA influences the cell–material interaction, the aim of this study was to evaluate the effects of electrochemically deposited HA and Sr-HA on the adhesion of MSCs. The present study can throw light on how Sr-HA influences the cell–material interaction and provide important information to improve the process.

2 Materials and methods

2.1 Sample synthesis and characterization of the coatings

Commercially pure titanium plates (10 mm× 10 mm×1 mm) and disks (diameter 20 mm and thickness 1 mm) were roughened as previously described (Liu *et al.*, 2011). In brief, they were first polished by SiC paper, sandblasted by SiC particles at a pressure of 4 MPa, and then ultrasonically cleaned with ethanol, acetone, and deionized water, in sequence. The titanium disks were immersed in a solution with 0.2% (v/v) HF and 0.4% (v/v) HNO_3 for 10 min at room temperature before they were in a solution with 25% (v/v) HCl and 25% (v/v) H_2SO_4 for 30 min at 80 °C. Subsequently, they were sprayed with water and then washed ultrasonically with deionized water before they were dried by nitrogen gas.

HA and Sr-HA coatings were synthesized by electrochemical deposition (Zhao S.F. *et al.*, 2013). Titanium disks were used as the working electrodes to deposit HA and Sr-HA while platinum plates were used as the counter electrode. Analytical-grade chemicals of $CaCl_2$, $NH_4H_2PO_4$, and $SrCl_2{\cdot}6H_2O$ were used as the Ca^{2+}, PO_4^{3-}, and Sr^{2+} sources, respectively. For HA, $CaCl_2$ and $NH_4H_2PO_4$ were dissolved in distilled water to form the electrolytes with the concentration of Ca^{2+} 1.2 mmol/L and of PO_4^{3-} 0.72 mmol/L. For Sr-HA, $SrCl_2{\cdot}6H_2O$ was distilled, and the concentration of Ca^{2+}+Sr^{2+} was 1.2 mmol/L with the $Sr^{2+}/(Sr^{2+}+Ca^{2+})$ molar ratio of 10%. In order to improve conductivity, 0.1 mol/L $NaNO_3$ was added to the solution. The deposition was performed using a direct-current (DC) power source operated at 3.0 V at 85 °C for 1 h.

Field-emission scanning electron microscopy (FESEM) was used to examine the morphologies of the coatings. Contact angles were measured using the static sessile drop method using a face contact angle set-up equipped with a camera to determine the hydrophilicity. X-ray diffraction (XRD) and X-ray photoelectron spectroscopy (XPS) were used to conduct the phase analysis of the synthesized coatings.

2.2 Cell cultures

The animals used in this research were treated as approved by the Institutional Animal Care and Use Committee of Zhejiang University, Hangzhou, China. MSCs were obtained from 4-week-old rats. The detailed cell isolation procedures are described elsewhere (Zhao *et al.*, 2012). The cells were cultured in Eagle's alpha minimum essential medium (MEM) supplemented with 10% (v/v) fetal bovine serum and antibiotics (penicillin 100 U/ml and streptomycin 100 μg/ml) at 37 °C in a humidified atmosphere incubator with 5% CO_2/95% air, and the medium was refreshed every 3 d.

2.3 Cell morphology

The cells of passages 3–5 were used in the experiments. The samples of size 10 mm×10 mm×1 mm were placed in 24-well plates, and MSCs were seeded on each sample at a density of 3×10^4 cells/well. After culturing for 1, 6, and 24 h, the samples were washed with phosphate-buffered saline (PBS) three times, and fixed in 2.5% (v/v) glutaraldehyde for 1 h. Then the samples were dehydrated by a series of graded alcohols, and dried by critical point drying before they were gold-sputtered. Finally, their cell morphology and attachment of the cells on each surface were analyzed with FESEM.

2.4 Cell viability

3-(4,5-Dimethylthiazol-2-yl)-2,5-diphenyltetrazolium bromide (MTT) assay was used to determine the metabolic condition of the cells (Ni *et al.*, 2011). After culturing for 1, 6, and 24 h, MTT (5 mg/ml) (Sigma Aldrich, St. Louis, MO, USA) was added to each well and the cells were cultured for another 4 h. After the culture medium was removed, 100 μl dimethyl sulfoxide (DMSO; Sigma Aldrich) was added to the well and oscillated for 10 min. Then the absorbance at 490 nm was measured each well. Each group contained three samples.

2.5 Cytoskeleton structure and cell adhesion

After the samples were incubated for 1, 6, and 24 h, they were rinsed with the PBS three times to remove the non-attached cells. Subsequently, they were fixed in 4% (v/v) paraformaldehyde at room temperature for 30 min, and washed again with PBS three times before they were permeabilized with 0.1% (v/v) Triton X-100 for 10 min, and washed three more times with PBS. The samples were incubated in bovine serum albumin blocking agent (1%) for 30 min. Fluorescein isothiocyanate (FITC)-phalloidin (5 μg/ml) (Sigma Aldrich) was added to the samples before they were incubated at 37 °C for 60 min. Subsequently, the samples were washed three times with PBS and incubated in Hoechst 33258 (1 μg/ml; Beyotime, Shanghai, China) for 3 min at room temperature. After the samples were rinsed with PBS three times, they were added with anti-fade fluorescence mounting medium. Then the samples were analyzed with a fluorescence microscopy to randomly capture images of three areas on a sample. The images were studied using the ImageJ software to count the number of adherent cell nuclei. The average number of adherent cell nuclei was calculated.

2.6 Gene expression by real-time PCR analysis

Gene expression of vinculin, FAK, integrin β1, and integrin β3 of the MSCs cultured on Sr-HA-, HA-coated titanium disks and the roughened surface after 24, 48, and 72 h was evaluated using quantitative real-time reverse transcription polymerase chain reaction (RT-qPCR). Total RNA was isolated from the MSCs cultured at each time point using the TRIzol reagent according the manufacturer's instructions. One microgram of total RNA from the cells on each sample was reversed-transcribed into complementary DNA using PrimeScript™ RT Master Mix (Perfect Real Time). RT-qPCR for gene expression of vinculin, integrin β1, integrin β3, and FAK was performed in 96-well plates using a CFX Connect real-time system with RealMasterMix (Probe). The primer sequences are listed in Table 1. Data analysis was carried out using Bio-Rad CFX Manager. *β-Actin* was used as the housekeeping gene. The RT-qPCR was run in a CFX Connect real-time system using universal thermal cycling parameters. Quantitative analyses were carried out using the recommended software (Bio-Rad CFX Manager). Each sample was run in triplicates.

2.7 Statistical analysis

All analysis results are expressed as mean± standard deviation (SD). The data were analyzed using SPSS 14.0. At each point, a one-way analysis of variance (ANOVA) test was carried out to determine

Table 1 Rat gene primer sequences for RT-PCR

Gene	Sequence (5'→3')
Vinculin	F: GATGCTGGTGAACTCAATGA
	R: CGAATGATCTCGTTAATCTC
Integrin β1	F: AAGTGGGACACGGGTGAAAA
	R: AGAGCCCCAAAGCTACCCTA
Integrin β3	F: TGACCCGCTTCAATGACGAA
	R: ATGGGTCTTGGCATCAGTGG
FAK	F: CCAGGACGGTCTGTGTTTCA
	R: CATCGCTCCGACAGCATTTG
β-Actin	F: GCAGGAGTACGATGAGTCCG
	R: ACGCAGCTCAGTAACAGTCC

the statistical significance. A P-value of <0.05 was considered to be significant, and a P-value of <0.01 was considered to be highly significant.

3 Results

3.1 Synthesis and structure characterization

Figs. 1a and 1b show the SEM micrographs of the titanium surfaces after being sandblasted and treated with acids. The surface texture comprised pits, with each pit formed from many micropits. After electrochemical deposition, homogeneous coatings were synthesized on to the roughened surfaces. The porous morphology of the titanium surface can still be observed. These coatings were characterized by rod-like crystallites with a hexagonal cross section (Figs. 1c and 1d). When the Sr^{2+} was incorporated, the crystallites had a smaller diameter (Figs. 1e and 1f).

The measured contact angles of water droplets on the roughed surface, HA and Sr-HA are 40.5°±1.4° (n=9), 5.8°±0.6° (n=9), and 4.1°±1.1° (n=9), respectively. There was a significant difference between the roughened surface and the HA and Sr-HA. This indicated that the nanorod-structure could improve hydrophilicity compared to the roughened surface.

Table 2 shows the atomic percentage of Ca, P, C, O, and Sr in each coating. The majority of elements of the HA and Sr-HA coatings were Ca, P, C, and O, while Sr can only be detected in the Sr-HA coating with the atomic percentage of 0.67%.

The typical XRD patterns of different synthesized coatings are shown in Fig. 2. This confirmed that the deposits were composed of HA crystallites, and Sr was incorporated into the HA. With the addition of Sr element, the diffraction peaks shifted to lower 2θ values, which indicates an increase in lattice parameters. The crystallinity of HA decreased, as evidenced by the broadening of the HA diffraction peaks. However, the peak positions have not changed,

Table 2 Atomic percentages of Ca, P, O, C, and Sr in the HA and Sr-HA coatings using XPS test

Atom	Atomic percentage (%)	
	HA	Sr-HA
Ca	10.18	6.89
P	12.23	9.57
O	26.45	25.06
C	39.25	42.58
Sr	0	0.67

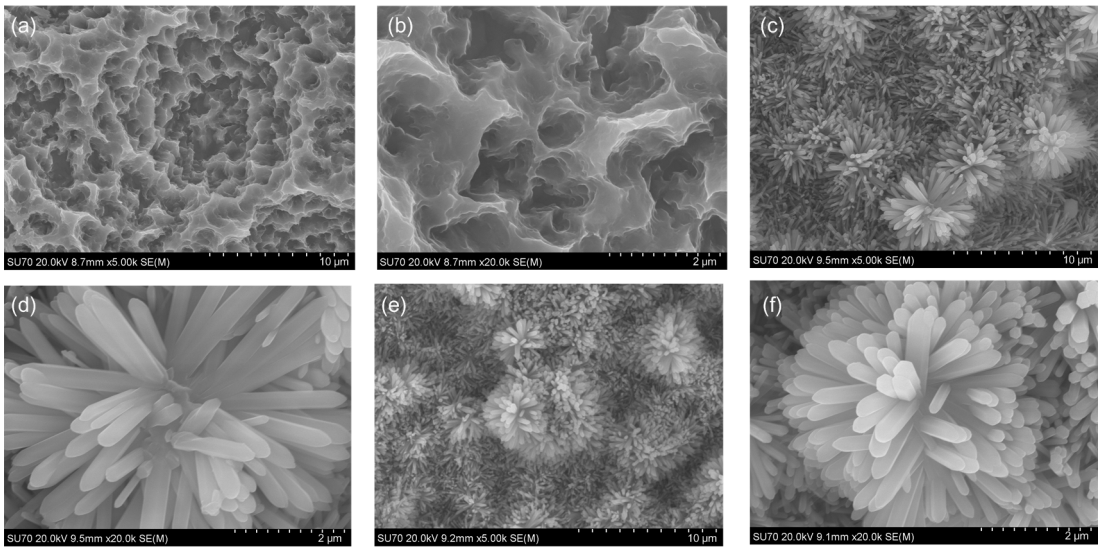

Fig. 1 SEM micrographs of the roughened surfaces (a, b), HA surfaces (c, d), and Sr-HA surfaces (e, f)
The porous structures appeared on the roughened surface

which indicates that the amount of Sr substitution was very small.

3.2 Cell adhesion and viability

Fig. 3a shows the number of MSCs on different titanium surfaces after 1, 6, and 24 h of incubation. The number of cells increased markedly with the time of incubation. At each time point, the number of adherent cells was found to be significantly higher on the Sr-HA- and HA-coated surfaces than on the roughened surface. However, the number of the cells adhering to the HA coating and Sr-HA coating showed no significant difference at 1 and 6 h. After incubation for 6 and 24 h, all coatings to some extent showed an increase in the number of the adherent cells. As shown in Fig. 3b, the MTT assay shows the same trend as the counting assay. The metabolic activity of adherent cells on the Sr-HA and HA coatings was much higher than that on the roughened surface, demonstrating that Sr-HA and HA coatings had no toxicity on MSCs and had a marked impact on the proliferation at the early period. The results also indicate that Sr-HA and HA coatings had better biocompatibility than the roughened titanium surface.

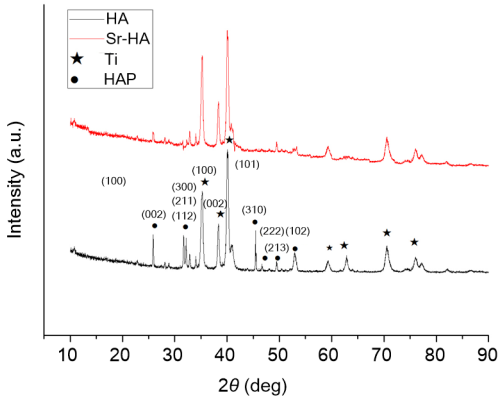

Fig. 2 XRD patterns of HA and Sr-HA coatings
a.u.: arbitrary unit; deg: degree (°); Ti: titanium; HAP: hydroxyapatite

3.3 Cell morphology

All groups displayed healthy adherent cells on titanium surfaces, as shown in Fig. 4. At 1 h, there was significant difference in cell morphology on all surfaces. Cells did not spread completely on the roughened surface. Only a few short cytoplasmic bridges of MSCs could be observed on the HA-coated surface. Cells on the Sr-HA surface exhibited a well-spread morphology with many cytoplasmic bridges across the crystallites and had a polymorphic shape. However, the cell shapes changed dramatically after 24 h of spreading. On the roughened surface, the cells presented as flattened structures with a distinct, spread morphology; however, the cells on HA and Sr-HA surfaces were distributed over the coatings and formed cytoplasmic bridges of variable thickness, suspended above the peaks and depressions. Compared to the roughed surface, HA and Sr-HA surfaces presented numerous protoplasmic processes of MSCs.

3.4 Fluorescence staining of MSCs' cytoskeleton

Fluorescence staining was performed to analyze the effects of the titanium surfaces on the MSCs' cytoskeleton, as shown in Fig. 5. On HA and Sr-HA

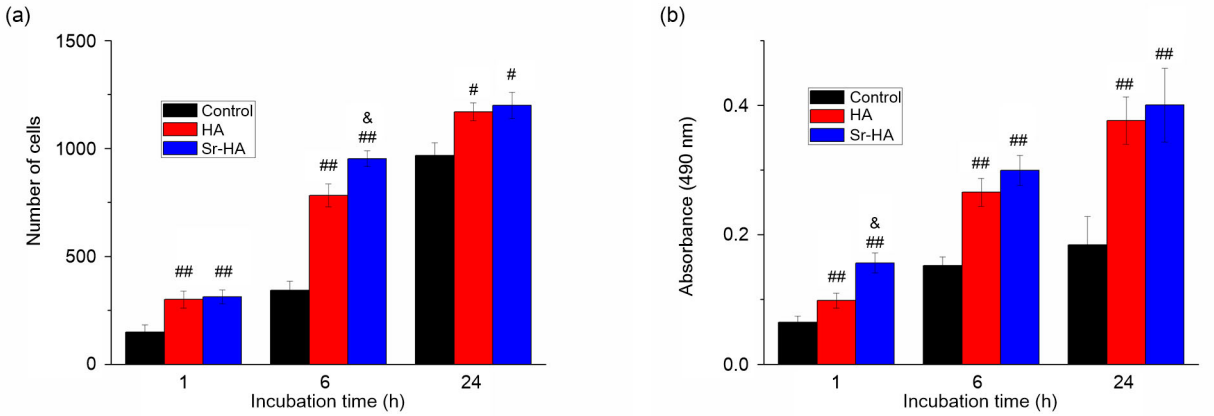

Fig. 3 Counting (a) and MTT (b) assays of MSCs cultured on roughened titanium surface, HA coating, and Sr-HA coating after 1, 6, and 24 h of incubation
Data are expressed as mean±SD with n=9. $^{\#\#}$ P<0.01, $^{\#}$ P<0.05, compared with the roughened titanium surface (control); $^{\&\&}$ P<0.01, $^{\&}$ P<0.05, compared with the HA

surfaces, the FITC-conjugated, phalloidin-stained MSCs revealed distinct and well-defined stress fibers and actin-containing micro-filaments after 24 h of culture (Figs. 5d and 5f). The cells on the roughened surface displayed weakly and poorly structured actin filaments (Fig. 5b). Cell–cell contacts and numerous filapodia-like processes were observed on all groups after 24-h incubation; however, they were not obvious after 1-h incubation (Figs. 5a, 5c, and 5e).

3.5 Effects of different coatings on gene expression of integrin β1, integrin β3, FAK, and vinculin

To investigate the effect of MSCs' adherence on the Sr-HA surface, the gene expression of integrin β1, integrin β3, FAK, and vinculin was analyzed using biochemical and molecular approaches. As shown in Fig. 6, at each time point the mRNA expression of integrin β1, integrin β3, FAK, and vinculin in cells was substantially upregulated on Sr-HA coating

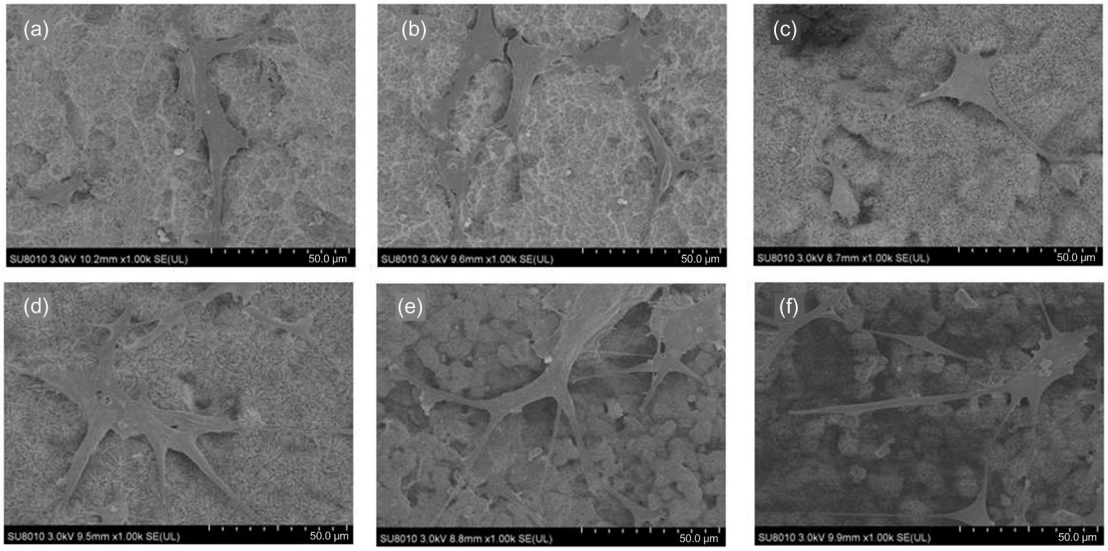

Fig. 4 SEM images of MSCs' adherence and morphology on the roughened surface (a, b), HA (c, d) and Sr-HA (e, f) coatings after 1 h (a, c, e) and 24 h (b, d, f) of incubation

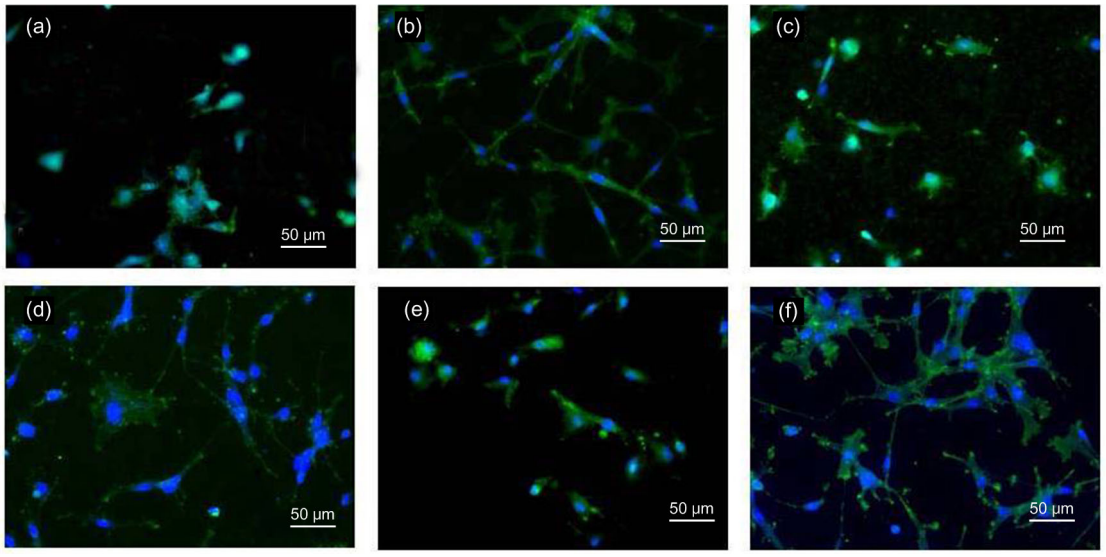

Fig. 5 Actin (green) and nucleus (blue) fluorescence images of MSCs on the roughened surface (a, b), HA (c, d) and Sr-HA (e, f) coatings after 1 h (a, c, e) and 24 h (b, d, f) of incubation

compared to MSCs cultured on roughened surfaces. At 24 h, the HA group also had a significantly higher gene expression levels of integrin β1, vinculin, and FAK compared to the roughened group, though integrin β1 showed no significant difference at 48 and 72 h between HA and the roughened surface. At 72 h, the gene levels of integrin β3 and vinculin showed no differences between HA and Sr-HA surfaces.

4 Discussion

In our present study, we produced nanostructed HA and Sr-HA coatings on a titanium surface using an electrochemical process and investigated the MSC adhesion to the different coatings. The results showed that the process successfully produced a thin coating on the porous titanium surface, and the Sr-HA coating evidently enhanced the adhesion of rat MSCs at the early stage compared to the roughened surface and HA coating.

With the purpose to further improve the bone implant contact as compared to using pure HA, Sr-doped calcium phosphate coatings on titanium surface have been prepared using different methods. The Sr-doped HA coating can be prepared by compression molding technique, plasma spraying technique, wet chemical synthesis, hydrothermal preparation, sol-gel route, and other means (Wong *et al.*, 2009; Abert *et al.*, 2014; Cox *et al.*, 2014; Xu *et al.*, 2014; Omar *et al.*, 2015). They reported that with the incorporation of Sr into HA, not only the mechanical properties but also the bioactivity of the samples was improved. The electrochemical deposit method has been used in our study to produce a Sr-doped HA coating on the roughened surface. These coatings were characterized by oriented rod-like crystallites with a hexagonal cross section. The coatings have high crystallinity

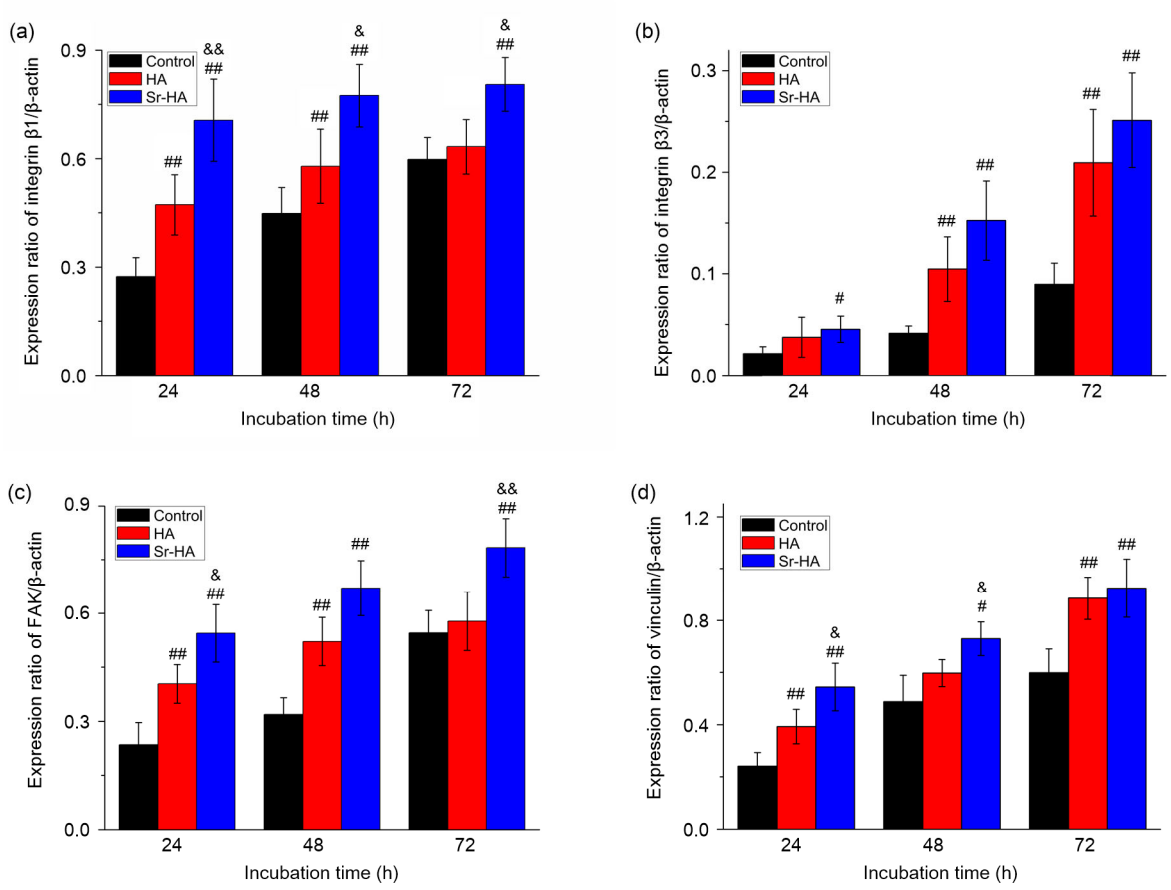

Fig. 6 Integrin β1 (a), integrin β3 (b), FAK (c), and vinculin (d) gene expression of MSCs on roughened titanium surface, HA coating, and Sr-HA coating after 24, 48, and 72 h of incubation

Data are expressed as mean±SD with n=9. $^{\#\#}$ P<0.01, $^{\#}$ P<0.05, compared with the roughened titanium surface (control); $^{\&\&}$ P<0.01, $^{\&}$ P<0.05, compared with the HA

and high wettability with decreased contact angle. The chemical structure of the coating can be controlled by changing the pH, temperature, and composition of the electrolyte, as well as the current density and deposit time. This technique did not destroy the porous surface of the titanium and the porous morphology of the titanium surface was still visible after electro-chemical deposition, because the coating was very thin. Moreover, the rod-like Sr-HA produced by this process was similar to the natural HA in bone, which was important for osseointegration.

Cell adhesion to a biomaterial is achieved via the formation of focal adhesion. The focal adhesion markers, vinculin and FAK (focal adhesion kinase) can be used to identify FA (focal adhesion) contact and the cytoskeleton. The characterization of FA can provide evidence on how topography affects cell adhesion (Seo *et al.*, 2013). When cells arrive at the titanium surface, they express a variety of integrins and bind to intracellular linker proteins of focal adhesion such as vinculin on one side and to extracellular anchoring ligands on the other side (Lim *et al.*, 2007; Yim *et al.*, 2010; Madamanchi *et al.*, 2014). In our present study, we found that the Sr-HA surface could greatly promote the gene expression levels of FAK, vinculin, integrin β1, and integrin β3 in the early stage of the MSC adhesion, and their levels increased with time. Krause *et al*. (2000) suggested that the integrin signaling is responsible for surface-dependent osteoblastic maturation. Knockdown of the integrin β1 in osteoblasts impairs the ability to recognize micro structured titanium surfaces. The results of fluorescence staining showed that on HA and Sr-HA surfaces, the FITC-conjugated, stress fibers and actin-containing micro-filaments were detected after 24 h of incubation. Cell–cell contacts and numerous filapodia-like processes were visible in all 24-h samples, but were not clearly seen in 1-h samples. The high gene expression can result in cytoskeletal changes. The changes in cytoskeletal tension have a direct effect on cell morphology, as evidenced by actin staining (Wang *et al.*, 2013). It has been confirmed that a highly organized cytoskeleton with stress fibers is associated with strong cell adhesion and, if the cell–material adhesion is weak, it fails to spread or form any stress fibers (Zhuang *et al.*, 2014). One possible reason for the results in our study is that when Sr is incorporated into HA, the structure of HA is altered, with the diameter of the crystallites becoming much smaller and the crystallites become closer to that of natural HA in the bone. The Sr-HA coating in this study endows the titanium surface with higher wettability and a decreased contact angle. A 3D nanotopography, when compared to the roughened surface, shows enhancement of the cellular attachment and direct modulation of cell adhesion and subsequently mediation of the secretion of anchoring proteins and the formation of focal adhesion (Park *et al.*, 2012; Aina *et al.*, 2013; Guo *et al.*, 2013; Kaygili *et al.*, 2015; Lindahl *et al.*, 2015). The other reason is that Sr, like calcium, acts as a receptor. The XRD results indicated that Sr-HA has higher crystallinity than the HA. Sr-HA also has higher solubility which leads to an elevated level of local ions, which can facilitate cell adhesion via a calcium-sensing-receptor-dependent mechanism (Hurtel-Lemaire *et al.*, 2009; Takaoka *et al.*, 2010; Kaygili *et al.*, 2015; Yang *et al.*, 2015). Previous studies showed that Sr promotes osteoblast replication and differentiation by activating the calcium sensing receptor (CaR), and the indicated downstream pathways in osteoblastic cells, resulting in increased osteoblastogenesis (Hurtel-Lemaire *et al.*, 2009; Takaoka *et al.*, 2010). Sr also activates the CaR and downstream signaling pathways in osteoclasts, causing reduced osteoclast differentiation and decreased bone resorption. The in vitro study of MSCs' adhesion on the different surfaces revealed that the metabolic activity and cell proliferation on the Sr-HA surface were upregulated in the early stage, indicating that the Sr-HA coating has better biocompatibility than the roughened and HA surfaces, which is consistent with previous studies (Zhou *et al.*, 2014; Lindahl *et al.*, 2015; Tao *et al.*, 2016a; 2016b).

Attachment, adhesion, and spreading in the early period of cell–material interaction are critical for modulating the capacity of a cell to proliferate and differentiate (Anselme, 2000). We found that changes in cytoskeletal tension of MSCs in response to topography of Sr-HA coating modified actin organization and thereby influenced the gene expression of FAK, vinculin, integrin β1, and integrin β3, which indicated that enhanced cell adhesion could be achieved on the Sr-HA surface. Further studies should be carried out to investigate whether and how Sr-HA coating enhances osteogenic differentiation of MSCs.

5 Conclusions

This study demonstrated the influence of an electrochemically deposited nanostructured Sr-HA-coated titanium surface on the adhesive behavior of MSCs. Cell proliferation, adhesion, cell morphology, and cytoskeleton structure were all upregulated considerably by the titanium surface modified with Sr-HA coating compared to the roughened surface. Our present work provides insights into the surface modification of the titanium implant favoring cell adhesion.

Compliance with ethics guidelines

Dan-li FU, Qiao-hong JIANG, Fu-ming HE, and Bai-ping FU declare that they have no conflict of interest.

All institutional and national guidelines for the care and use of laboratory animals were followed.

References

Abert, J., Bergmann, C., Fischer, H., 2014. Wet chemical synthesis of strontium-substituted hydroxyapatite and its influence on the mechanical and biological properties. *Ceram. Int.*, **40**(7):9195-9203. http://dx.doi.org/10.1016/j.ceramint.2014.01.138

Aina, V., Bergandi, L., Lusvardi, G., *et al.*, 2013. Sr-containing hydroxyapatite: morphologies of HA crystals and bioactivity on osteoblast cells. *Mater. Sci. Eng. C Mater. Biol. Appl.*, **33**(3):1132-1142. http://dx.doi.org/10.1016/j.msec.2012.12.005

Anselme, K., 2000. Osteoblast adhesion on biomaterials. *Biomaterials*, **21**(7):667-681. http://dx.doi.org/10.1016/S0142-9612(99)00242-2

Brammer, K.S., Choi, C., Frandsen, C.J., *et al.*, 2011. Hydrophobic nanopillars initiate mesenchymal stem cell aggregation and osteo-differentiation. *Acta Biomater.*, **7**(2):683-690. http://dx.doi.org/10.1016/j.actbio.2010.09.022

Branemark, P.I., 1983. Osseointegration and its experimental background. *J. Prosth. Dent.*, **50**(3):399-410. http://dx.doi.org/10.1016/S0022-3913(83)80101-2

Braux, J., Velard, F., Guillaume, C., *et al.*, 2011. A new insight into the dissociating effect of strontium on bone resorption and formation. *Acta Biomater.*, **7**(6):2593-2603. http://dx.doi.org/10.1016/j.actbio.2011.02.013

Cox, S.C., Jamshidi, P., Grover, L.M., *et al.*, 2014. Preparation and characterisation of nanophase Sr, Mg, and Zn substituted hydroxyapatite by aqueous precipitation. *Mater. Sci. Eng. C Mater. Biol. Appl.*, **35**:106-114. http://dx.doi.org/10.1016/j.msec.2013.10.015

Dalby, M.J., Gadegaard, N., Oreffo, R.O., 2014. Harnessing nanotopography and integrin-matrix interactions to influence stem cell fate. *Nat. Mater.*, **13**(6):558-569. http://dx.doi.org/10.1038/nmat3980

Fage, S.W., Muris, J., Jakobsen, S.S., *et al.*, 2016. Titanium: a review on exposure, release, penetration, allergy, epidemiology, and clinical reactivity. *Contact Dermat.*, **74**(6):323-345. http://dx.doi.org/10.1111/cod.12565

Fu, D.L., Jiang, Q.H., He, F.M., *et al.*, 2012. Fluorescence microscopic analysis of bone osseointegration of strontium-substituted hydroxyapatite implants. *J. Zhejiang Univ.-Sci. B (Biomed. & Biotechnol.)*, **13**(5):364-371. http://dx.doi.org/10.1631/jzus.B1100381

Gao, J., Wang, M., Shi, C., *et al.*, 2016. Synthesis of trace element Si and Sr codoping hydroxyapatite with non-cytotoxicity and enhanced cell proliferation and differentiation. *Biol. Trace Element Res.*, **174**(1):208-217. http://dx.doi.org/10.1007/s12011-016-0697-0

Guo, D.G., Hao, Y.Z., Li, H.Y., *et al.*, 2013. Influences of Sr dose on the crystal structure parameters and Sr distributions of Sr-incorporated hydroxyapatite. *J. Biomed. Mater. Res. Part B Appl. Biomater.*, **101**(7):1275-1283. http://dx.doi.org/10.1002/jbmb.32940

Hurtel-Lemaire, A.S., Mentaverri, R., Caudrillier, A., *et al.*, 2009. The calcium-sensing receptor is involved in strontium ranelate-induced osteoclast apoptosis. New insights into the associated signaling pathways. *J. Biol. Chem.*, **284**(1):575-584. http://dx.doi.org/10.1074/jbc.M801668200

Jiang, Q.H., Gong, X., Wang, X.X., *et al.*, 2015. Osteogenesis of rat mesenchymal stem cells and osteoblastic cells on strontium-doped nanohydroxyapatite-coated titanium surfaces. *Int. J. Oral Maxillofac. Implants*, **30**(2):461-471. http://dx.doi.org/10.11607/jomi.3798

Jiao, M.J., Wang, X.X., 2009. Electrolytic deposition of magnesium-substituted hydroxyapatite crystals on titanium substrate. *Mater. Lett.*, **63**(27):2286-2289. http://dx.doi.org/10.1016/j.matlet.2009.07.048

Kaneko, K., Ito, M., Naoe, Y., *et al.*, 2014. Integrin αv in the mechanical response of osteoblast lineage cells. *Biochem. Biophys. Res. Commun.*, **447**(2):352-357. http://dx.doi.org/10.1016/j.bbrc.2014.04.006

Kaygili, O., Keser, S., Kom, M., *et al.*, 2015. Strontium substituted hydroxyapatites: synthesis and determination of their structural properties, in vitro and in vivo performance. *Mater. Sci. Eng. C Mater. Biol. Appl.*, **55**: 538-546. http://dx.doi.org/10.1016/j.msec.2015.05.081

Khang, D., Choi, J., Im, Y.M., *et al.*, 2012. Role of subnano-, nano- and submicron-surface features on osteoblast differentiation of bone marrow mesenchymal stem cells. *Biomaterials*, **33**(26):5997-6007. http://dx.doi.org/10.1016/j.biomaterials.2012.05.005

Krause, A., Cowles, E.A., Gronowicz, G., 2000. Integrin-mediated signaling in osteoblasts on titanium implant materials. *J. Biomed. Mater. Res.*, **52**(4):738-747. http://dx.doi.org/10.1002/1097-4636(20001215)52:4<738::AID-JBM19>3.0.CO;2-F

Krishna, O.D., Jha, A.K., Jia, X., *et al.*, 2011. Integrin-mediated adhesion and proliferation of human MSCs

elicited by a hydroxyproline-lacking, collagen-like peptide. *Biomaterials*, **32**(27):6412-6424. http://dx.doi.org/10.1016/j.biomaterials.2011.05.034

Kumar, A., Nune, K.C., Basu, B., *et al.*, 2016. Mechanistic contribution of electroconductive hydroxyapatite-titanium disilicide composite on the alignment and proliferation of cells. *J. Biomater. Appl.*, **30**(10):1505-1516. http://dx.doi.org/10.1177/0885328216631670

Kuo, S.W., Lin, H.I., Ho, J.H., *et al*., 2012. Regulation of the fate of human mesenchymal stem cells by mechanical and stereo-topographical cues provided by silicon nanowires. *Biomaterials*, **33**(20):5013-5022. http://dx.doi.org/10.1016/j.biomaterials.2012.03.080

Lee, J., Chu, B.H., Chen, K.H., *et al.*, 2009. Randomly oriented, upright SiO_2 coated nanorods for reduced adhesion of mammalian cells. *Biomaterials*, **30**(27):4488-4493. http://dx.doi.org/10.1016/j.biomaterials.2009.05.028

Lim, J.Y., Dreiss, A.D., Zhou, Z., *et al.*, 2007. The regulation of integrin-mediated osteoblast focal adhesion and focal adhesion kinase expression by nanoscale topography. *Biomaterials*, **28**(10):1787-1797. http://dx.doi.org/10.1016/j.biomaterials.2006.12.020

Lindahl, C., Pujari-Palmer, S., Hoess, A., *et al.*, 2015. The influence of Sr content in calcium phosphate coatings. *Mater. Sci. Eng. C Mater. Biol. Appl.*, **53**:322-330. http://dx.doi.org/10.1016/j.msec.2015.04.015

Liu, J., Wang, X.D., Jin, Q.M., *et al*., 2012. The stimulation of adipose-derived stem cell differentiation and mineralization by ordered rod-like fluorapatite coatings. *Biomaterials*, **33**(20):5036-5046. http://dx.doi.org/10.1016/j.biomaterials.2012.03.050

Liu, L., Song, L.N., Yang, G.L., *et al.*, 2011. Fabrication, characterization, and biological assessment of multilayer DNA coatings on sandblasted-dual acid etched titanium surface. *J. Biomed. Mater. Res. Part A*, **97A**(3):300-310. http://dx.doi.org/10.1002/jbm.a.33059

Loya, M.C., Brammer, K.S., Choi, C., *et al.*, 2010. Plasma-induced nanopillars on bare metal coronary stent surface for enhanced endothelialization. *Acta Biomater.*, **6**(12): 4589-4595. http://dx.doi.org/10.1016/j.actbio.2010.07.007

Madamanchi, A., Santoro, S.A., Zutter, M.M., 2014. α2β1 Integrin. *Adv. Exp. Med. Biol.*, **819**:41-60. http://dx.doi.org/10.1007/978-94-017-9153-3_3

Matschegewski, C., Staehlke, S., Loeffler, R., *et al.*, 2010. Cell architecture-cell function dependencies on titanium arrays with regular geometry. *Biomaterials*, **31**(22):5729-5740. http://dx.doi.org/10.1016/j.biomaterials.2010.03.073

Ni, G.X., Yao, Z.P., Huang, G.T., *et al.*, 2011. The effect of strontium incorporation in hydroxyapatite on osteoblasts in vitro. *J. Mater. Sci. Mater. Med.*, **22**(4):961-967. http://dx.doi.org/10.1007/s10856-011-4264-0

Omar, S., Repp, F., Desimone, P.M., *et al.*, 2015. Sol–gel hybrid coatings with strontium-doped 45S5 glass particles for enhancing the performance of stainless steel implants: electrochemical, bioactive and *in vivo* response. *J. Non-Crystal. Solids*, **425**:1-10. http://dx.doi.org/10.1016/j.jnoncrysol.2015.05.024

Park, J.H., Wasilewski, C.E., Almodovar, N., *et al.*, 2012. The responses to surface wettability gradients induced by chitosan nanofilms on microtextured titanium mediated by specific integrin receptors. *Biomaterials*, **33**(30):7386-7393. http://dx.doi.org/10.1016/j.biomaterials.2012.06.066

Park, J.K., Kim, Y.J., Yeom, J., *et al.*, 2010. The topographic effect of zinc oxide nanoflowers on osteoblast growth and osseointegration. *Adv. Mater.*, **22**(43):4857-4861. http://dx.doi.org/10.1002/adma.201002255

Peng, S., Zhou, G., Luk, K.D., *et al.*, 2009. Strontium promotes osteogenic differentiation of mesenchymal stem cells through the Ras/MAPK signaling pathway. *Cell. Physiol. Biochem.*, **23**(1-3):165-174. http://dx.doi.org/10.1159/000204105

Seo, C.H., Jeong, H., Furukawa, K.S., *et al.*, 2013. The switching of focal adhesion maturation sites and actin filament activation for MSCs by topography of well-defined micropatterned surfaces. *Biomaterials*, **34**(7): 1764-1771. http://dx.doi.org/10.1016/j.biomaterials.2012.11.031

Shi, J., Dong, L.L., He, F., *et al.*, 2013. Osteoblast responses to thin nanohydroxyapatite coated on roughened titanium surfaces deposited by an electrochemical process. *Oral Surg. Oral Med. Oral Pathol. Oral Radiol.*, **116**(5):e311-e316. http://dx.doi.org/10.1016/j.oooo.2012.02.021

Sirin, H.T., Vargel, I., Kutsal, T., *et al.*, 2015. Ti implants with nanostructured and HA-coated surfaces for improved osseointegration. *Artif. Cells Nanomed. Biotechnol.*, **44**(3):1023-1030. http://dx.doi.org/10.3109/21691401.2015.1008512

Sisti, K.E., de Andres, M.C., Johnston, D., *et al.*, 2015. Skeletal stem cell and bone implant interactions are enhanced by LASER titanium modification. *Biochem. Biophys. Res. Commun.*, **473**(3):719-725. http://dx.doi.org/10.1016/j.bbrc.2015.10.013

Takaoka, S., Yamaguchi, T., Yano, S., *et al.*, 2010. The calcium-sensing receptor (CAR) is involved in strontium ranelate-induced osteoblast differentiation and mineralization. *Horm. Metab. Res.*, **42**(9):627-631. http://dx.doi.org/10.1055/s-0030-1255091

Tao, Z.S., Bai, B.L., He, X.W., *et al.*, 2016a. A comparative study of strontium-substituted hydroxyapatite coating on implant's osseointegration for osteopenic rats. *Med. Biol. Eng. Comput.*, **54**(12):1959-1968. http://dx.doi.org/10.1007/s11517-016-1494-9

Tao, Z.S., Zhou, W.S., He, X.W., *et al.*, 2016b. A comparative study of zinc, magnesium, strontium-incorporated hydroxyapatite-coated titanium implants for osseointegration of osteopenic rats. *Mater. Sci. Eng. C Mater. Biol. Appl.*, **62**:226-232. http://dx.doi.org/10.1016/j.msec.2016.01.034

Uccelli, A., Moretta, L., Pistoia, V., 2008. Mesenchymal stem

cells in health and disease. *Nat. Rev. Immunol.*, **8**(9): 726-736.
http://dx.doi.org/10.1038/nri2395

Wang, W., Zhao, L., Wu, K., *et al.*, 2013. The role of integrin-linked kinase/β-catenin pathway in the enhanced MG63 differentiation by micro/nano-textured topography. *Biomaterials*, **34**(3):631-640.
http://dx.doi.org/10.1016/j.biomaterials.2012.10.021

Wong, K.L., Wong, C.T., Liu, W.C., *et al.*, 2009. Mechanical properties and in vitro response of strontium-containing hydroxyapatite/polyetheretherketone composites. *Biomaterials*, **30**(23-24):3810-3817.
http://dx.doi.org/10.1016/j.biomaterials.2009.04.016

Xu, J., Yang, Y., Wan, R., *et al.*, 2014. Hydrothermal preparation and characterization of ultralong strontium-substituted hydroxyapatite whiskers using acetamide as homogeneous precipitation reagent. *Sci. World J.*, **2014**: 863137.
http://dx.doi.org/10.1155/2014/863137

Yang, F., Yang, D., Tu, J., *et al.*, 2011. Strontium enhances osteogenic differentiation of mesenchymal stem cells and in vivo bone formation by activating Wnt/Catenin signaling. *Stem Cells*, **29**(6):981-991.
http://dx.doi.org/10.1002/stem.646

Yang, H.W., Lin, M.H., Shang, G.W., *et al*., 2015. Osteogenesis of bone marrow mesenchymal stem cells on strontium-substituted nano-hydroxyapatite coated roughened titanium surfaces. *Int. J. Clin. Exp. Med.*, **8**(1):257-264.

Yim, E.K., Darling, E.M., Kulangara, K., *et al.*, 2010. Nanotopography-induced changes in focal adhesions, cytoskeletal organization, and mechanical properties of human mesenchymal stem cells. *Biomaterials*, **31**(6): 1299-1306.
http://dx.doi.org/10.1016/j.biomaterials.2009.10.037

Zhao, L., Liu, L., Wu, Z., *et al.*, 2012. Effects of micropitted/nanotubular titania topographies on bone mesenchymal stem cell osteogenic differentiation. *Biomaterials*, **33**(9): 2629-2641.
http://dx.doi.org/10.1016/j.biomaterials.2011.12.024

Zhao, L., Wang, H., Huo, K., *et al.*, 2013. The osteogenic activity of strontium loaded titania nanotube arrays on titanium substrates. *Biomaterials*, **34**(1):19-29.
http://dx.doi.org/10.1016/j.biomaterials.2012.09.041

Zhao, S.F., Dong, W.J., Jiang, Q.H., *et al.*, 2013. Effects of zinc-substituted nano-hydroxyapatite coatings on bone integration with implant surfaces. *J. Zhejiang Univ.-Sci. B (Biomed. & Biotechnol.)*, **14**(6):518-525.
http://dx.doi.org/10.1631/jzus.B1200327

Zhao, S.F., Shi, J., He, F.M., *et al.*, 2014. Design and in vitro evaluation of simvastatin-hydroxyapatite coatings by an electrochemical process on titanium surfaces. *J. Biomed. Nanotechnol.*, **10**(7):1313-1319.
http://dx.doi.org/10.1166/jbn.2014.1859

Zhou, J., Li, B., Lu, S., *et al.*, 2013. Regulation of osteoblast proliferation and differentiation by interrod spacing of Sr-HA nanorods on microporous titania coatings. *ACS Appl. Mater. Interf.*, **5**(11):5358-5365.
http://dx.doi.org/10.1021/am401339n

Zhou, J., Han, Y., Lu, S., 2014. Direct role of interrod spacing in mediating cell adhesion on Sr-HA nanorod-patterned coatings. *Int. J. Nanomed.*, **9**:1243-1260.
http://dx.doi.org/10.2147/IJN.S58236

Zhuang, X.M., Zhou, B., Ouyang, J.L., *et al.*, 2014. Enhanced MC3T3-E1 preosteoblast response and bone formation on the addition of nano-needle and nano-porous features to microtopographical titanium surfaces. *Biomed. Mater.*, **9**(4):045001.
http://dx.doi.org/10.1088/1748-6041/9/4/045001

中文概要

题　目：多孔纯钛表面掺锶羟基磷灰石涂层对骨髓间充质干细胞粘附的影响

目　的：观察电化学沉积的纳米结构掺锶羟基磷灰石涂层表面对大鼠骨髓间充质干细胞早期粘附行为的影响。

创新点：首次观察电化学沉积的掺锶羟基磷灰石涂层表面骨髓间充质干细胞的早期粘附行为，并对相关基因进行了检测。

方　法：纯钛表面经过喷砂和双重酸处理，形成多孔粗糙结构。用电化学方法在其粗糙表面沉积羟基磷灰石涂层（HA）和掺锶羟基磷灰石涂层（Sr-HA）。用贴壁法将 4 周大鼠股骨骨髓间充质干细胞分离进行原代培养后将细胞接种到多孔纯钛，HA 和 Sr-HA 表面培养 1、6 和 24 小时。用场发射扫描电镜（SEM）观察细胞的形貌特点。用异硫氰酸荧光素（FITC）标记的鬼笔环肽进行免疫荧光染色标记细胞骨架，Hoechst 33258 进行细胞核染色，激光共聚焦荧光显微镜进行拍照后使用 ImageJ 进行细胞的计数和图形分析。用实时荧光定量逆转录聚合酶链式反应（RT-qPCR）测定 24、48 和 72 小时不同实验组中骨髓间充质干细胞中 FAK、vinculin、integrin β1 和 integrin β3 的基因表达，并进行统计学分析。

结　论：SEM 观察结果显示，骨髓间充质干细胞在三种表面都能正常黏附、生长和增殖。在 Sr-HA 组表面，细胞粘附、细胞活力和细胞骨架的铺展都较粗糙表面组和 HA 组有较显著的提高。RT-qPCR 结果显示，在各个时间点 Sr-HA 组表面骨髓间充质干细胞的 FAK、vinculin、integrin β1 和 integrin β3 的基因表达与粗糙组有显著性差异，且在 24 小时后与 HA 组亦有显著性差异。综上所述，掺锶羟基磷灰石纳米涂层具有较好的生物相容性，可以促进大鼠骨髓间充质干细胞在纯钛表面的早期粘附。

关键词：细胞粘附；骨髓间充质干细胞；掺锶羟基磷灰石；钛